Title of Investigation: Studies of Solar Activity with Coordinated Observations of New Solar Telescope and NASA Solar Physics Missions

Principal Investigator: Philip Goode, BBSO/NJIT

Co-Principal Investigators: Wenda Cao and Haimin Wang

Proposal Summary

I HAVE CUT DOWN IT A LOT, STILL TOO LONG, 300 WORDS IS THE LIMIT

In the last 2 years since the start of our prior SRT grant, Big Bear Solar Observatory (BBSO) has remained highly productive – both scientifically and in the development of requisite instrumentation. This productivity includes graduating 8 Ph.D.s and producing over 60 publications. BBSO has reached the final stage in building its 1.6 meter clear aperture, off-axis New Solar Telescope (NST). First-light of this telescope is expected in Spring 2008. All of these efforts are well-time and focussed to support important current and near future NASA missions including RHESSI, Hinode, STEREO and SDO.

Under the support of this new grant, we will be integrating visible and near infrared vector magnetograph systems with the NST, and will carry out advanced commissioning of the NST bringing it up to its full scientific capability.

Our primary targets of our scientific research are:

1. High-cadence and high-resolution studies of solar flare emissions. These observations will provide unique details of flare energy precipitation on 0.2" spatial scales and 0.1 sec temporal scales. These studies bear on, and will enhance RHESSI and Hinode research.

2. Sustained sub-arc second resolution studies of the quiet solar atmosphere. (a) We will observe and directly probe the newly discovered transverse magnetic component, which is weaker than intranetwork fields. (b) We will address the energy source of coronal heating, from high-resolution observations of footpoint motiona of flux ropes. NST is complementary to Hinode and SDO in this study.

3. Comprehensive studies of vector magnetic fields associated with flares, to understand the triggering mechanism of the eruptions and atmospheric restructuring after the eruptions. NST is complementary to Hinode, STEREO and SDO in this study.

4. Study of flow fields in flare productive active regions using near-continuous high-resolution, high-cadence observations. NST is complementary to Hinode and SDO here.

The proposed research is clearly related to the NASA's strategic goal 3B: to understand the sun and its effects on Earth.

A. Project Description

A.1 Results from Prior NASA-SR&T Support (Feb. 2006 to Jan. 2008)

New Jersey Institute of Technology (NJIT) took over operation of Big Bear Solar Observatory (BBSO) on July 1, 1997. On Feb. 1, 2006, our current three-year SR&T grant started. This grant is one of two backbone grants supporting BBSO. BBSO has been one of two solar observatories in the US with a telescope, instrumentation and a site that enables diffraction limited studies of the Sun with a half-meter class telescope. The other is the National Solar Observatory (NSO) with its somewhat larger aperture Dunn Solar Telescope. This upper limit on aperture for high-resolution solar observations is about to radically change. BBSO will soon be observing with its 1.6 m clear aperture New Solar Telescope (NST) with adaptive optics (AO) and state-of-the-art polarimeters in the visible and near-infrared (NIR). Further, over the next decade, NSO will be building the Advanced Technology Solar Telescope (ATST) in Hawaii. The 4 m off-axis, ATST will benefit from its NST predecessor, which is also off-axis. The NST will dominate U.S. ground-based observations until the middle of the next decade. After the ATST is online, the NST will still have an essential role for the community because the NST will be the large aperture solar telescope working in sustained campaigns – essential for the broadly-based, high-resolution observations needed to gather unique data to understand the fundamental nature of solar magnetism and its evolution. Our capability of running sustained campaigns has been at the core of our ability to provide unique support to the community's efforts to study and understand the Sun, especially providing data that will be complementary to those from RHESSI, STEREO, Hinode and SDO. Observing campaigns are essential to determine the origin of "space weather", which arises from solar magnetic storms and can impact Earth. Since 1997, we have made systematic, fundamental changes in the observatory's instrumentation to ensure a unique and significant scientific role for BBSO. The advances in instrumentation were critical for improving the quality of our observations. We devoted considerable effort to instrument development

up to, and including the NST, and the resulting improvements in data quality helped our research group to be even more productive, as evidenced by over 60 publications in the two years since Feb. 2006.

NJIT continues to strongly support our efforts, and would match this grant with $300 K for new equipment for the observatory. It is also fully funding two lead staff positions for the NST and beyond - the Project Director (Roy Coulter) and the Optical Engineer (Nicolas Gorceix).

BBSO highly prizes its special role in the education of the next generation of scientists who build instruments. We graduated 8 Ph.D.'s from 2006 to 2007. We currently have 6 Ph.D. students (5 men and 1 woman). Most of our recent Ph.D.s are very active in solar physics research. Since the beginning of our current SR&T support, three of our post-docs have advanced to tenure-track faculty positions in the U.S.. Wenda Cao is now an assistant professor at NJIT. Jiong Qiu is an assistant professor at Montana State University. Deqing Ren is an assistant professor at California State University, Northridge. Over the last decade, six other former BBSO/NJIT post-docs have earned professorships outside of the US.

BBSO has an unpaid, outside Advisory Board, which meets bi-annually to critique our efforts. The Board's report is made to BBSO management and passed on to the upper management of NJIT. The current members of the board are Len Fisk (University of Michigan, Chair), Ken Libbrecht (Caltech), Jeff Kuhn (University of Hawaii), and Spiro Antiochos (Naval Research Lab). We respect their advice and use it to improve the observatory.

Since NJIT began operating BBSO, its telescope time and data have been open to the community. Many scientists have had observing time. Students from around the world are using BBSO data as a central part of the work on their theses. Data requests come to BBSO on a daily basis from around the world. Since the summer of 2002, a substantial part of our data has been available in near real-time on the web *http://www.bbso.njit.edu*. We also have implemented an internal fiber optic link and a RAID array for our FTP archive. For users of our telescopes and data, we only ask that they acknowledge BBSO in their resulting publications. Many observers use our data to help plan their observing campaigns.

BBSO achievements in instrumentation will be included in the on-going instrumentation section, while for the remainder of this section, we focus on the highlights of some of our scientific achievements under current SR&T support. Our publications, in the form of BBSO Bluebooks, are also available on our website.

A.1.1 High Cadence Flare Observations

In 2004, Ji et al. (2004a) discovered that flare ribbons may first contract before their normal expansion. Ji et al. (2006) obtained more comprehensive results from a high-cadence (40 ms) Hα blue-wing observation of an M1.1-class solar flare, which occurred in NOAA AR 10687 on November 1, 2004. Such studies also agree with recent RHESSI results; e.g., the ones presented by Veronig et al. (2006), Sui and Holman (2003), Sui et al. (2004), all showing some sort of loop contraction before the main phases of the eruptions. These phenomena are not well-understood within existing flare models. However, these observations motivate theorists to revisit the various flare models with new and powerful constraints.

A.1.2 Rapid Evolution of Magnetic Fields Associated with Flares

In recent years, we presented a series of new observational result showing rapid changes in sunspot structure associated with a substantial fraction of flares (Wang et al. 2004a; Deng et al. 2005; Liu et al. 2005, Chen et al., 2007). In particular, Liu et al. (2005) studied the relationship between the changes in δ-spot structures and associated major flares for seven events. The results were quite consistent for all the events: part of the penumbral segments in the outer δ-spot structure decayed rapidly after a major flare; meanwhile, the neighboring umbral cores and/or inner penumbral regions became darker. The rapid changes, which can be identified in the time profiles of white-light (WL) mean intensity, are permanent, not transient, and thus are not due to flare emission. In the two events for which vector magnetograms were available, we found a decrease in the transverse field in areas of penumbral decay, while the field and area increased in the central darkened regions. Both events also show an increase in the magnetic shear after the flares. To explain these observations, we proposed a reconnection picture in which the two components of a δ-

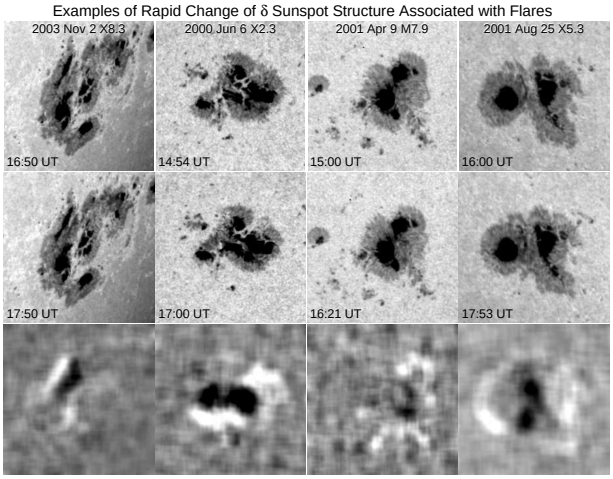

Figure 1: TRACE WL images revealing the rapid change of δ sunspot structure associated with four major flares. The top, middle, and bottom rows show the pre-flare images, post-flare images, and the difference images between them, respectively. The white feature in the difference images indicates the region of penumbral decay, while the dark feature indicates the region of central umbral/penumbral enhancement (Adapted from Liu et al. 2005).

spot become strongly connected after the flare. The penumbral fields change from a highly inclined to a more vertical configuration, which implies penumbral decay. The umbral core and inner penumbral region become darker as a result of increasing longitudinal and transverse magnetic field components. Figure 1 shows examples of the rapid changes in sunspot structure described above; the difference between pre- and post-flare images is that the flaring neutral line is darkened, while a bright ring appears corresponding to the penumbral decay in the peripheral penumbrae.

Wang (2006) found that obvious changes in the magnetic gradient occurred, immediately and rapidly, following the onset of each flare. In addition, we evaluated the mean relative motion between the two magnetic polarities in these δ regions, in the directions parallel to, and perpendicular to the flaring neutral lines, respectively. Using a method of Center of Mass (CoM) calculation, we found that: (1) Converging motion corresponds to a gradient increase, while diverging motion corresponds to a decrease. (2) For all events, there appeared a sudden release of magnetic shear associated with each flare, signified by a decrease in the CoM separation of between 500 and 1,200 km in the direction parallel to the neutral lines. Combining the findings as presented in several papers, we proposed that these are evidence of magnetic reconnection at, or close to the photosphere.

Furthermore, we presented results of a statistical study of rapid penumbral decay associated with over 400 flares (Chen et al. 2007). We found that the rapid structural change in sunspots is more likely to be detected when associated with large solar flares - the larger the flare magnitude, the larger the change. For X-class flares, 45% of events show distinct change. But for M- and C-class flares, this percentage drops to 16% and 10%, respectively. We suspect that the decrease of percentage arises from limitations in data precision from currently available instrumentation.

A.1.3 Relationship between Flares and Magnetic Reconnection

Jing et al. (2007) investigated the spatial distribution of the hard X-ray intensity along flare ribbons and compared it with the local magnetic reconnection rate and energy release rate predicted by the standard magnetic reconnection model for two ribbon flares. In the early phase of the flare, the hard X-ray sources appear to be concentrated in strong field regions within the Hα ribbons, which is explicable by the model. At, and after the maximum phase of a flare, the hard X-ray sources become spatially extended to resemble Hα ribbons in morphology, during which the spatial distribution of hard X-ray intensity lacks a correlation with that of the local magnetic reconnection rate and the energy release rate predicted by the model. We argue that the magnetic reconnection during this event may involve the rearrangement of magnetic field along the magnetic arcade axis, which is inevitably overlooked in the two-dimensional model and suggests that this type of three-dimensional reconnection will be best seen in so-called "sigmoid-to-arcade transformations".

Liu et al. (2007) found that the flare brightening starts in the core of the active region earlier than the rising motion of the flux rope. This timing clearly addresses one of the main issues in the magnetic eruption onset of sigmoid, namely, whether the eruption is initiated by an internal tether cutting that allows the flux rope to rise upward, or a flux rope rises due to a loss of equilibrium to later induce tether cutting below it. Our high time cadence SXI and Hα data show that

the first scenario is relevant to such eruptions. As in other major findings, we have the RHESSI HXR images showing a change of the HXR source from a confined footpoint structure to an elongated ribbon-like structure after the flare maximum, which we relate to the sigmoid-to-arcade evolution. These various observed properties seem best interpreted with the runaway tether-cutting model proposed by Moore et al. in 2001.

A.1.4 Selected BBSO Publications from February 2006 to January 2008

The discussion above sketches some highlights of our scientific accomplishments over the past two years. Beyond those, and due to limited space, we list only selected publications (25 of 60) from the period of our present SR&T support. Please check the home page (`solar.njit.edu/preprints`) for a complete list with downloadable copies.

BBSO 1270: *High Resolution Observations of Multi-Wavelength Emissions during Two X-Class White-Light Flares*, Yan Xu, Wenda Cao, Chang Liu, Guo Yang, Ju Jing, Carsten Denker, Haimin Wang, Gordon Emslie, 2006, Ap.J., 641, 1210

BBSO 1273: *Relationship Between Magnetic Gradient and Magnetic Shear in Five Super Active Regions Producing Great Flares*, Haimin Wang, Hui Song, Ju Jing, Vasyl Yurchyshyn, Yuan-Yong Deng, Hong-Qi Zhang, David Falconer, Jing Li, 2006, ChJAA 6, 477

BBSO 1281: *Large-Scale Activities Associated with the 2003 October 28 X10 Flare*, Chang Liu, Jeongwoo Lee, Na Deng, Dale E. Gary, Haimin Wang, 2006, Ap.J. , 642, 1205

BBSO 1286: *Multiwavelength Study of Flow Fields in Flaring Super Active Region NOAA 10486*, Na Deng, Yan Xu, Guo Yang, Wenda Cao, Chang Liu, Thomas R. Rimmele, Haimin Wang, Carsten Denker, 2006, Ap.J. 644, 1287

BBSO 1290: *Evidence for a Quadrupole Magnetic Configuration in the April 9 2001 M7.9 Flare as Inferred from Multi Wavelength Observations*, V. Yurchyshyn, M. Karlicky, Q. Hu, H. Wang, 2006, Solar Physics, 235, 147

BBSO 1294: *The Statistical Relationship Between the Photospheric Magnetic Parameters and the Flare Productivity of Active Regions*, Ju Jing, Hui Song, Valentyna Abramenko, Changyi Tan, Haimin Wang, 2006, Ap.J., 644, 1273

BBSO 1295: *The Automatic Predictability of Super Geomagnetic Storm from Halo CMEs Associated with Large Scale Solar Flares*, Hui Song, Vasyl Yurchyshyn, Guo Yang, Changyi Tan, Weizhong Chen, Haimin Wang, 2006, Solar Physics, 238, 141

BBSO 1299: *The Rate of Emergence of Magnetic Dipoles in Coronal Holes and Adjacent Quiet-Sun Regions*, V.I. Abramenko, L.A. Fisk, V.B. Yurchyshyn, 2006, Ap.J. Letters, 641, 65

BBSO 1309: *Coronal Heating and Photospheric Turbulence Parameters: Observational Aspects*, V.I. Abramenko, Alexei P. Pevtsov, R. Romano, 2006, Ap.J Letters., 646, L81

BBSO 1310: *Rapid Changes of Photospheric Magnetic Fields around Flaring Magnetic Neutral Lines*, Haimin Wang, 2006, Ap.J., 649, 490

BBSO 1311: *Adaptive Optics at the Big Bear Solar Observatory: Instrument Description and First Observations*, Carsten Denker, Alexandra Tritschler, Thomas R. Rimmele, Kit Richards, Steve L. Hegwer, Friedrich Woger, 2006, PASP, 119, 170

BBSO 1318: *Automatic Detection of Prominence Eruption Using Consecutive Solar Images*, Gang Fu, Frank Y. Shih, Haimin Wang, 2007, IEEE Trans. on Circuits and Systems for Video Technology, 17, 79-85

BBSO 1319: *Field Dependent Adaptive Optics Correction Derived with the Spectral Ratio Technique*, C. Denker, N. Deng, T.R. Rimmele, A. Tritschler, A. Verdoni, 2007, Solar Physics, 241, 411-426

BBSO 1321: *Diffraction-limited Polarimetry from the Infrared Imaging Magnetograph at Big Bear Solar Observatory*, Wenda Cao, Ju Jing, Jun Ma, Yan Xu, Haimin Wang, Philip R. Goode, 2006, PASP, 118, 838

BBSO 1322: *First Light of the Near-Infrared Narrow-Band Tunable Birefringent Filter at Big Bear Solar Observatory*, Wenda Cao, Klaus Hartkorn, Jun Ma, Yan Xu, Tom Spirock, Haimin Wang, Philip R. Goode, Solar Physics, 2006, 238, 207

BBSO 1325: *The Ribbon-Like Hard X-Ray Emission in a Sigmoidal Solar Active Region*, Chang Liu, Jeongwoo Lee, Dale E. Gary, Haimin Wang, 2007, Ap.J., 658, L127

BBSO 1331: *The Relaxation of Sheared Magnetic Fields - A Contracting Process*, Haisheng Ji, Guangli Huang, Haimin Wang, 2007, Ap.J., 660, 893

BBSO 1332: *Filament Eruption after the Onset of the X1.5 Flare on 2005 September 13*, Haimin Wang, Chang Liu, Ju Jing, Vasyl Yurchyshyn, 2007, Ap.J., 671, 973-977

BBSO 1340: *Statistical Correlations between Parameters of Photospheric Magnetic Fields and Coronal Soft X-ray Brightness*, Changyi Tan, Ju Jing, V.I. Abramenko, A.A. Pevtsov, Hui Song, Sung-Hong Park, Haimin Wang, 2007, Ap.J. 660, 1460-1468

BBSO 1342: *Hard X-Ray Intensity Distribution Along Hα Ribbons*, Ju Jing, Jeongwoo Lee, Chang Liu, Dale E. Gary and Haimin Wang, 2007, Ap.J. Letters, 664, L127-130

BBSO 1343: *The Eruption from a Sigmoidal Solar Active Region on 2005 May 13*, Chang Liu, Jeongwoo Lee, Vasyl Yurchyshyn, Na Deng, Kyung-Suk Cho, Marian Karlicky and Haimin Wang, 2007, Ap.J., 669, 1372-1381

BBSO 1348: *Flow Field Evolution of a Decaying Sunspot*, Na Deng, Debi Prasad Choudhary, Alexandra Tritschler, Carsten Denker, Chang Liu and Haimin Wang, 2007, Ap.J., 671, 1013-1021

BBSO 1350: *Relationship between EIT Post Eruption Arcades, Coronal Mass Ejections, Coronal Neutral Line and Magnetic Clouds*, Vasyl Yurchyshyn, 2007, GRL, submitted

BBSO 1352: *Spatial Distribution of Magnetic Reconnection in the 2006 December 13 Solar Flare as Observed by Hinode*, Ju Jing, Jongchul Chae and Haimin Wang, 2008, Ap.J. Letters, 672, L73

BBSO 1353: *The Spatial Distribution of Hard X-Ray Spectral Index and Local Magnetic Reconnection Rate*, Chang Liu, Jeongwoo Lee, Ju Jing, Dale E. Gary and Haimin Wang, 2008, Ap.J. Letters, 672, L77-80

B. Proposed Research

The research we propose here is built on our long experience, but with the excitement and anticipation of a new solar telescope with three times the aperture of the old solar telescope. The NST is the culmination of a decade of re-instrumentation at BBSO. The NST will enable us to probe, spatially and temporally, phenomena that have been tantalizingly just beyond our grasp. Before proposing the first science that will take advantage of the NST, we give a brief overview of the instruments that will make the science possible.

B.1 Current Instrumentation Projects

B.1.1 New Solar Telescope (NST) with Adaptive Optics (AO)

The 1.6 m off-axis NST is the central instrumentation project at BBSO at this time. The telescope is nearing completion with system integration to begin in Big Bear in the Spring of 2008, and engineering first light in the Summer of 2008. We anticipate a year long "commissioning" phase during which we will be able to make evermore sophisticated observations with the NST. A key reason that we expect the NST commissioning to be shorter than one might first guess is that the essential downstream hardware has already been used to make successful scientific observations. The first light scientific observations will occur in the NIR early in the commissioning phase at the Nasmyth bench, which is affixed to the outside of the primary mirror cell. The NST should be operational, in a basic mode, by the beginning of funding from this proposal.

The new, larger dome, required to house the NST, is fully operational and all construction under the dome (such as the extension of the support pier) has been completed and awaits the telescope. The off-axis, 1.7 m primary mirror (PM), which will yield a 1.6 m clear aperture telescope, is undergoing final touch-ups at Steward Observatory Mirror Lab, while the elliptical secondary mirror (SM) is finished and silvered. The PM is active, and its shape will be controlled by an off-the-shelf wavefront sensing system, which will reside after the SM. The heat stop is completed. The opening in the heat stop defines the $150'' \times 150''$ field of view of the NST. The Optical Support Structure (OSS) is being built by DFM Engineering, Inc. of Longmont, CO and will be installed in Big Bear during March 2008. The first draft of the BBSO telescope headquarters control system software has been written and is undergoing testing in Big Bear and Longmont. This software is not required for early, first light scientific observations because we can use the mature control software from DFM.

In parallel with the NST development, we modified the AO system (primarily a newly designed optical feed) to operate with the NST, which feeds corrected light to our visible light (VIM) and NIR (IRIM) Fabry-Pérot based polarimeters. The light for the AO, VIM and IRIM is fed through the telescope's polar axis to the temperature controlled Coudé Laboratory on the floor beneath, where all of this hardware has been successfully used with light from the old 0.6 m telescope. Parts of the VIM and IRIM hardware can also function at the Nasmyth bench (mounted on the outside of the mirror cell of the primary), but with tip/tilt rather than full AO corrections. This bench will ultimately be very useful in far IR studies of the solar atmosphere. Infrared spectroscopy and spectropolarimetry at wavelengths longer than 2.5 μm remain largely unexplored, especially at the high spatial resolution, which will be afforded by the NST. Imaging and spectroscopy of the CO molecular line profiles at high resolution will constrain current models (Wedemeyer et al., 2005) of the coolest gas in the quiet Sun. Spectroscopy and polarimetry of the 2.2 μm Ti I lines currently provide the most sensitive magnetic probe in sunspot umbrae, but Si I lines at 4 μm may be twice as sensitive (the exact transition and thus magnetic sensitivity still remains unknown). Finally, chromospheric lines from Ca I near 4 μm (where the BBSO mean Fried parameter should be about 0.6 m) have very high magnetic sensitivity and may revolutionize our understanding of the chromospheric magnetic field; this will be very important for magnetic extrapolation models of the photospheric vector fields.

We had successfully operated our AO system on BBSO's old 0.6 m telescope. The AO system is characterized by a 97 element deformable mirror and Shack-Hartmann sensor, which samples the telescope

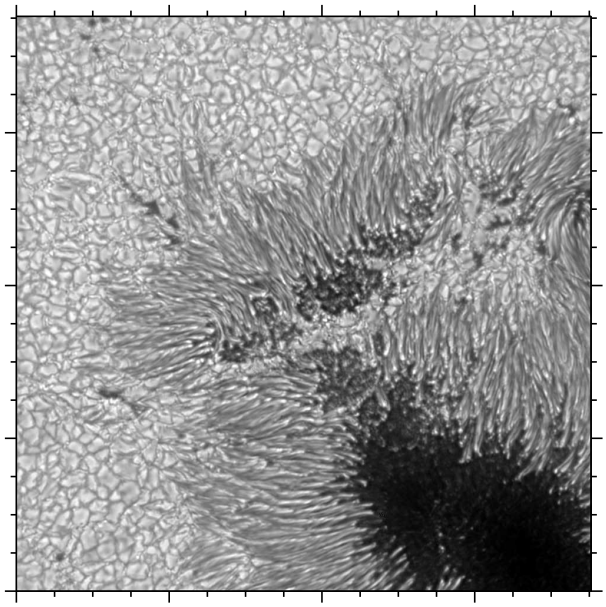

Figure 2: A diffraction-limited image obtained at BBSO on April 29, 2005 with the AO-76 system and speckle reconstruction.

entrance aperture with 76 lenslet elements. Hence, its name "AO-76". A number of papers have been published to describe this AO system (and its twin at NSO), as well as the scientific results (Ren et al., 2003; Didkovsky et al., 2003; Denker et al., 2005; Rimmele, 2004; Yang et al., 2004; Denker et al., 2007; Xu et al., 2004, 2006). Figure 2 shows a sample image obtained on April 29, 2005 with the BBSO AO system.

The practical experience from the DST, BBSO and other adaptive optics solar telescopes shows that Strehl ratios of S $\geq$ 0.3 are required in the detector plane to obtain reliable quantitative results from spectroscopic and polarimetric AO corrected observations. Forward modeling using MHD simulations combined with radiative transfer and modeled AO Point-Spread-Functions provide simulated observations that can be used to determine the "ground truth" of the MHD simulations. Such comparison indicate that, in particular because of the extended nature of the observed object, high Strehl ratios (S $\geq$ 0.3) are required to obtain reliable quantitative measurements of the solar structure. In particular, polarimetric observations with low Strehl range from difficult to impossible to interpret. The problem here is that the requisite opposite polarity measurements are often closely (tenths of arcsecs) spaced together.

AO-76 used in the NST will be able to provide diffraction limited sustained images in the NIR, but only rarely in the visible. The ATST site survey report showed BBSO has a median Fried parameter (measure of largest diffraction limited aperture without correction being needed) of about 6 cm at 0.5 μm, which translates to about 24 cm in the NIR at 1.6 μm. Forward modeling (Rimmele, 2008, private communication) using MHD simulations combined with radiative transfer and modeled AO Point-Spread-Functions provide simulated observations that can be used to determine that under nominal BBSO seeing conditions the Strehl ratio would be about 0.8 at 1 μm in the detector plane. the "ground truth" of the MHD simulations. Such modeling also indicates, in general, that because of the extended nature of the Sun, high Strehl ratios (S $\geq$ 0.3) are required to obtain reliable quantitative measurements of the solar structure. In particular, polarimetric observations with low Strehl range from difficult to impossible to interpret. The problem here is that the requisite opposite polarity measurements are often closely (tenths of arcsecs) spaced together. To achieve the full science capability of the NST in visible light observations, we are seeking separate funding (from NSF) to build an AO system around a commercially available 349 element DM ("AO-308"). Our calculations show that this DM will deliver the requisite mean Strehl of 0.3 in the detector plane. Thus, for our purposes here, we will concentrate on the NIR.

B.1.2 Focal Plane Instrumentation

The IRIM system developed by BBSO is in operation (Cao et al., 2006). It is one of the first imaging spectropolarimeters working at 1565 nm, and is used for observations of the Sun at its opacity minimum, exposing the deepest photospheric layers that can be seen. IRIM is a tandem system, which includes a 4.2 nm interference filter, a unique 0.25 nm birefringent Lyot filter, and a Fabry-Pérot etalon. IRIM is capable of providing a bandpass as low as 0.01 nm in a telecentric configuration. Benefiting from our correlation tracking system and our AO-76 system that have been adapted to the NST for first light observations. Implementing AO-76 on the NST is a more straightforward proposition than it was on the old telescope that was never meant for an adaptive optics system. The first imaging polarimetric observa-

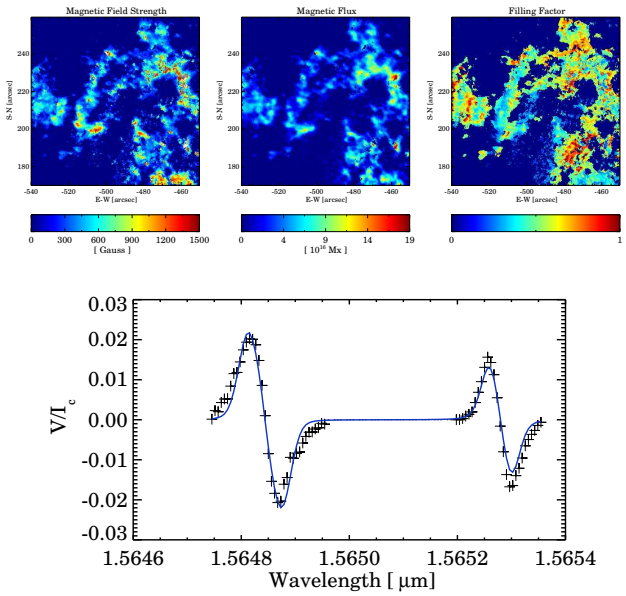

Figure 3: Sample result of IRIM observations with AO-76 at BBSO. It includes (a) true-field strength, (b) magnetic flux, and (c) filling factor maps of NOAA Active Region 10781 (Cao et al., 2006). The bottom plot is an example of Stokes-V fitting using the two prominent 1.6 μm NIR lines simultaneously.

tions at 1565 nm were made at the diffraction limit on July 1, 2005 using BBSO's old 0.6 m telescope. Stokes-V profiles were obtained from the Fabry-Pérot etalon scan, and the data provide access to both the true magnetic field strength and the filling factor of the small-scale magnetic flux elements. Figure 3 shows sample images obtained by IRIM and an example of the Stokes-V profile from the two adjacent NIR lines. The strength of the IRIM is its extreme sensitivity and high spatial resolution, which allows us to study weak and small-scale magnetic fields in the quiet Sun. In active regions, it enables accurate measurements avoiding Zeeman saturation of the traditional filter-based magnetograph systems. Both magnetic field strength and the filling factor were derived from fitting the Stokes V profiles (Cao et al., 2006). In parallel to the IRIM development, we have built a separate Visible Imaging Magnetograph (VIM) that has attained first light observations (Denker et al., 2007), which includes photometric and magnetogram data. Both magnetograph systems are prepared for integration into the NST.

We have programmed a 32-node parallel computing cluster, so that we can perform real-time speckle reconstruction with a cadence of about 1 minute (for a 1 K$\times$1 K camera). Diffraction limited images will be achieved all the time during the entire observing period. An upgrade of the system to carry out Blind Multi-Frame De-convolution and Phase-Diversity processing is underway. Before this instrument, speckle reconstruction of images would take hours of *post facto* processing to construct a single diffraction limited image (as in Denker and Wang, 1998). This effectively limited us to a short observing day ($\sim$ 2 hours) because the control computer's disk would be filled by storing all the raw data, so the chances were slim of obtaining a sequence containing the long term evolution of an active region, and catching flares during the observations. Even with a larger disk, we would still be left with an unwieldy processing problem.

B.1.3 Milestones in the Commissioning of the NST

We recognize that the integration of NST, AO and focal plane instruments is a laborious task, and that this is the first phase in the commissioning of the NST. However, we are confident that most of the system integration needed for what we propose will be accomplished before the start date of the proposal, for the following reasons: (1) Telescope alignment will be done in collaboration with a team of contracted, outside experts, which includes the UA Steward Observatory Mirror Lab with whom we are already working on this part of the project. (2) AO, IRIM, VIM and the real-time image reconstruction system are all operating hardware that have been tested and proven with the old 0.6 m telescope. To maximize the scientific return, we will adopt the concept of an on-going commissioning; i.e., ever-broadening scientific observations as the commissioning evolves. Table 1 lists the milestones of NST commissioning, and corresponding scientific observations. Please note that initial scientific operation will not be done with active mirror control, which is the most complicated component in the commissioning process. The effect of delayed active mirror control will put an additional burden on the AO.

Date	NST Milestone	Scientific Observations	Resolution
Spring 2008	Telescope Installation		
Summer 2008	Nasmyth First Light	Sunspot and plage structure in NIR	0.5″
Fall 2008	Light to Coudé Feed	Flare emission and magnetic fields in FIR	0.5″
Fall 2008	AO-76 Implemented	High resolution of atmosphere and magnetic fields	0.3″
Spring 2009	Active Mirror Control	Higher resolution observations	0.2″
After 2009	Begin AO-308 Project	Highest resolution observations in visible light	0.05″
After 2009	Nasmyth Far IR Spectrograph	Probe chromosphere with good resolution (@4μm)	0.5″

Table 1: Milestones in NST Commissioning

B.2 Proposed Scientific Research

Each proposed scientific research task takes advantage of one or more of the NST's unique attributes, which include high spatial and temporal resolution, precise measurements of vector magnetic fields and observations of faint features. We will probe what has been just beyond our grasp, but build on our earlier research. The proposed research is also very timely, as NASA missions Hinode, STEREO were launched in 2006, and SDO will be launched in the latter part of 2008. Joint observations between NST and these satellites will produce unprecedented scientific returns.

At 1.6 μm, where the IRIM is designed to utilize the two strong magnetic lines, the NST will have a spatial resolution of about 0.2″. One might ask what advantages are expected over data from the old 0.6 m aperture BBSO telescope, which also had a spatial resolution of 0.2″, but at 0.5 μm. First, the Zeeman splitting increases quadratically with wavelength, so the IRIM can more precisely detect magnetic flux. Second, we will now be able to separate out the true magnetic field strength and the filling factor for the small-scale magnetic flux elements, as shown in Figure 3. Third, the terrestrial atmosphere is more benign in the NIR with the mean Fried parameter at BBSO being about 25 cm (under the assumption of Komolgorov turbulence), which is four times that at 0.5 μm. This improvement is essential in the observations of faint features, which drift in and out of sharpness. The focal plane Strehl is sufficient to enable sustained diffraction limited images with AO-76 under typical BBSO observing conditions, but images at 0.5 μm would only be diffraction limited under extraordinary seeing conditions at BBSO. For this reason, we are planning AO-308, which will enable diffraction limited imaging in the detector plane in visible light. Fourth, the NST is a 2 m^2 "light-bucket" that will accumulate sufficient photons for very high temporal cadence observations of rapid phenomena.

B.2.1 Sub-arcsecond, Sub-second Structure of Flares

It was first discovered in high-resolution hard X-ray and microwave observations that flare bursts consist of fine structures changing on timescales from tens of milli-seconds to a few seconds (van Beek, de Feiter, & de Jager 1974, 1976; Hoyng, van Beek, & Brown 1976; Kiplinger et al. 1983, 1988; Kaufmann et al. 1980, 1984, 2001; Aschwanden, Benz & Schwartz, 1993; Aschwanden, Schwartz, & Alt, 1995; Aschwanden et al. 1995, 1998). These are the so-called "elementary bursts" (de Jager & de Jonge 1978). In recent years, efforts to search for small-scale structures have also been made in optical wavelengths, typically using Hα observations (Wang et al. 2000; Trottet et al. 2000; Kurt et al. 2000).

The discovery of temporal fine structures in flares has led scientists to consider that magnetic energy release occurs primarily on small-scales; e.g., Lu & Hamilton (1991) proposed the possibility that the coronal magnetic fields are in a self-organized critical state, and solar flares are avalanches of many small-scale events. In terms of a physical mechanism, the most popular belief is that solar flares comprise many small-scale reconnections (Sturrock et al. 1984; Parker 1989; Bastian & Valhos 1997). Formation of magnetic islands by tearing-instabilities and subsequent interactions between these magnetic islands, namely dynamic magnetic reconnection (Kliem et al. 2000 and references therein), are generally regards as accounting for the fast variations in non-thermal emissions on "elementary burst" timescales (Aschwanden 2002 and references therein).

Since 1999, we have carried out on-going, high-cadence flare-watch campaigns. We have looked in the far blue wing of the Hα line in an attempt to locate sites of non-thermal beam precipitation in the impulsive phase of solar flares. The campaigns have yielded fruitful results in high-resolution studies of flares and related phenomena (Wang et al. 2000; Qiu et al. 2000, 2001, 2002; Qiu & Wang, 2006; Ding et al. 2001; Wang & Qiu 2002; Ji et al., 2003, 2004a,b, 2006). However, these previous BBSO observations could

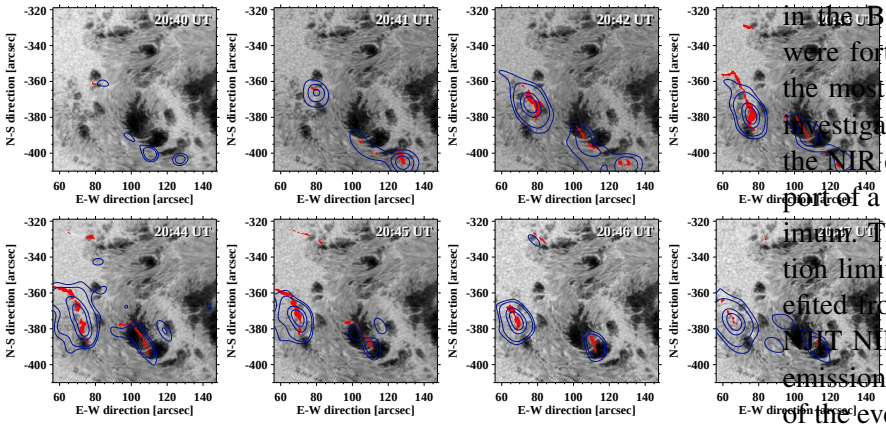

Figure 4: NIR time sequence (AO corrected) of the X10 flare from 20:40 UT to 20:47 UT on October 29, 2003. RHESSI HXR contours (blue) correspond to the 50 - 100 keV channel with 60 integrations. The local NIR intensity maxima are shown in red. Two flare ribbons are correlated with strong HXR kernels. HXR contour levels are drawn at 0.17, 0.25, 0.60, and 0.80 of the maximum intensity, except for the first two frames, where they correspond to 0.7 and 0.8 for the first frame and 0.4, 0.6, and 0.8 for the second, when the HXR kernels were weaker (Xu et al. (2004).

not resolve the spatial structure of flare emissions because the spatial resolution has a lower limit of about $1''$. *The NST will provide an unprecedented mapping of flaring with high temporal cadence, first with $0.2''$ resolution in the NIR, then downstream, with AO-308, below $0.1''$ in visible. These scales are anticipated to be the sizes of individual flux tubes.*

The observing lines/bands will be: 1.6 μm, He D3, Hα and He 10830. Each wavelength has its own merit in the diagnosis of flare electron precipitation. Most of our prior observations were in Hα off-band observations. However, we found that high-resolution/cadence observations at 1.6 μm can pin down the site(s) of electron precipitation, and many such events will be observed with high spatial resolution. Xu et al. (2004, 2006) discussed high-resolution observations of two white-light flares in solar active region NOAA 10486 obtained with the Dunn Solar Telescope (DST) at the National Solar Observatory/Sacramento Peak (NSO/SP) at the end of October 2003 when BBSO hardware was 'evacuated' to NSO/SP for several days due to a large forest fire in the Big Bear environs. During this interim, we were fortunate to record significant events in one of the most unusual active regions in many years. Our investigation focused on flare dynamics observed in the NIR continuum at 1.56 μm. This was the first report of a white-light flare observed at the opacity minimum. The spatial resolution was close to the diffraction limit of the 76 cm aperture DST. The data benefited from the newly developed AO system and the NJIT NIR camera. Figure 4 compares the NIR flare emissions with the hard X-ray data of RHESSI for one of the events.

NST observations combined with HXR data from RHESSI and high resolution magnetograms from Hinode, we expect to find: **(1) the characteristic timescale of elementary bursts, (2) simultaneity of the elementary bursts at the magnetically conjugate footpoints, (3) spatial scale of the elementary bursts**. *The NST with IRIM will make these observations possible because tracking these rapidly changing small features typically requires high spatial resolution with a high Strehl. This is at the heart of the technical reasons why there have been so few high-cadence flare observations.* Joint observations with RHESSI HXR and OVRO microwave will also reveal the electron distribution in these elementary bursts. Broadband NIR observations can be achieved immediately at the Nasmyth station. Polarimetric and spectroscopic properties of flare emission can be obtained when AO-76 correction is implemented in the Coudé Lab. Of course, other shorter wavelength observations mentioned above will further enhance the power of this study in the future, when the higher-order AO (DM with 349 actuators) is built.

As an added feature to the high-cadence, high-resolution flare studies, we will investigate the motion of flare footpoints. It is well-accepted that solar flares are due to the sudden release of magnetic energy in a magnetic reconnection (Forbes & Priest 1995). In the classical two-dimensional "CSHKP" reconnection model of a two-ribbon flare (Carmichael 1964; Sturrock 1966; Hirayama 1974; Kopp & Pneuman 1976), oppositely directed magnetic field lines are stretched by eruption to form a vertical current sheet where reconnection occurs. According to this model, the two footpoints (FPs) of a flare, residing in areas of opposite magnetic polarities, are expanding outward and away from each other as the flare proceeds (Svestka &

Cliver 1992). Furthermore, it is well-recognized that flare ribbon expansion is the chromospheric signature of progressive magnetic reconnection in the corona, in which new field lines reconnect at higher and higher altitudes. Recent ground-based observations, along with RHESSI observations, raise a challenging question to this classical physical picture: two flare ribbons seem to first come closer together, and then separate. The second part is predicted by the CSHKP model, while the first part is not even thought of in the model. Ji et al. (2004b) showed such inward motion was evident even for the individual flare peaks in a multi-peak event.

The explanation for the contracting motion of footpoints and loop-tops is in its preliminary stages. Ji et al. (2004b) proposed that they are caused by a pinching motion of the current sheet within the framework of the CSHKP model, in which the vertical current sheet is enhanced in the reconnecting region. Then in turn, the energy release rate is enhanced to produce HXR spikes, and the footpoints are pushed together; however, this picture cannot explain the drop in the altitude of the HXR loop-top source. On the other hand, Veronig et al. (2006) modelled a collapsing magnetic trap embedded in a standard 2D magnetic reconnection model. They can reproduce the altitude decrease of the flare X-ray loop-top and the observed RHESSI spectra. However, the inward motion of the footpoints is not predicted in this explanation. We also note the "implosion" picture proposed by Hudson (2000) may predict contracting loop-tops along with the inward motion of the footpoints. As pointed out by Hudson, the detection of such an implosion requires high-cadence, high-resolution observations of flare footpoints during the impulsive phase. Our observations are therefore uniquely suited to the purpose of understanding the basic physics by exploiting the NST's new generation observations of flares with high-cadence and high-resolution, which will be aided by RHESSI HXR imaging. In addition, quantitative analyses will provide important information for in-depth modelling.

Prior high-resolution observations of flares hardly exist at all. With a minimum of $0.2''$ spatial resolution and 100 ms cadence NST observations, we expect to answer the basic questions that have eluded us: **(1) The detailed trajectory of footpoint motion corresponding to individual flux tubes. (2) The relationship between the speed and magnitude of the inward motion and the energy release of the flares. (3) For each of the sub-peaks in a multi-peak flare, do we see the contracting motion that Ji et al. (2004b) found?** With beamsplitters, the observations will be done simultaneously in at least two wavelengths among Hα, He D3, 1.56 μm, and HeI 10830 with AO, so that we can achieve sufficiently high signal-to-noise to track footpoint motion.

B.2.2 High Resolution NIR Observations of the Non-Flaring Solar Atmosphere

Although our proposed research focuses on high-resolution observations of solar activity, *the NST will certainly provide unprecedented data to elucidate the dynamics of magnetic structures in the quiet atmosphere. In the initial phase of NST operation, the AO-76 system can routinely provide full correction in NIR only; therefore, our scientific initial objectives will be tied to this instrumental capability.*

In addition to the advantages of observing in the near IR listed at the beginning of **C.2.**, the Sun has an opacity minimum in the NIR (at about 1.6 μm). Thus, one can see deeper into the Sun at those wavelengths. For all these reasons, observations in the NIR would then result in significant steps forward in our understanding of the Sun, such as being able to make much more precise measurements of the magnetic field and its evolution. We will focus on the following two topics based on the recent scientific advances in these areas. The NST is coming at the right time to push these studies further.

C.2.2.1. Quiet Sun Magnetic Fields That Are Weaker than Intranetwork Fields

This specific scientific objective is motivated by a recent discovery by Harvey et al. (2007). They found that the photospheric magnetic field, outside of active regions and the network, has a ubiquitous and dynamic line-of-sight component that strengthens from disk center to limb as expected for a field of nearly horizontal orientation. A similar claim has been made with the initial Hinode results (Lites et al., 2008, Suarez et al., 2007). According to Harvey et al. (2007), this newly discovered magnetic component is not present in the chromosphere. Therefore, it is natural to search for its signature sampling the deepest photosphere. In the NIR the terrestrial at-

mosphere is more benign and IRIM samples down to about 50 km beneath the visible photosphere; therefore, it is highly likely that we will be able to observe and characterize this new magnetic component in the quiet Sun. Throughout the proposal, almost all the scientific goals will be achieved with our baseline polarization precision of 10^{-3}. However, because of the extremely weak signal of this magnetic component, we will push our polarization precision to be below 10^{-4} with IRIM. This accuracy is essential for measuring magnetic fields on the order of a few gauss. We will try several ways to achieve this, such as using a beam splitter to obtain the two polarizations simultaneously, and coupled with long integration. Such an observing mode will be used mainly for this topic.

C.2.2.2. Contribution of Footprint Motion to Coronal Loop Heating

Aschwanden et al. (2000) argued that for coronal loops, the heating is concentrated in the footpoints (at altitudes of 50 to 300 Mm). Although a heating function was given, the detailed heating mechanism was not described. Contrarywise, Priest et al. (2000) argued that coronal loops have uniform heating. We can address the controversy by focusing on a search for possible heating mechanisms near the footpoints. For the uniform loop heating model, Parker (1988) proposed that the X-ray corona is due to a continuous nanoflaring process. The energy source for these nanoflares is the random motion of footpoints. Furthermore, nanoflares, microflares, and even regular solar flares may be somehow associated (Hudson, 1991), so observations of footpoint motions associated with all the above types of events are essential. We know from experience that such footpoint motion is hard to observe and characterize in lower resolution ($1''$) magnetograph and filtergraph observations. In a recent study (Tan et al., 2007), we found that the energy of a proxy for Poynting flux ($E = \frac{1}{4\pi}|V_h| \cdot |B_z|^2$) ranges from $10^{6.7}$ to $10^{7.6}$ erg cm^{-2} s^{-1} for the majority of ARs, which is sufficient to heat the corona due to random motion of magnetic flux tubes footpoints in the photosphere. This Poynting flux has a good correlation with the coronal brightness as shown in Figure 5. *Our previous efforts had two limitations: (1) the velocity observations were based on tracking of MDI magnetograms, and the resulting errors are high. (2) The transverse magnetic field measurements were not available, so the proxy (line-of-sight field) that we used may not have been valid. Obviously, NST observations will overcome both limitations.* With those barriers overcome, we can accurately derive the dynamic properties of small-scale magnetic fields and their contribution to coronal heating. In particular, local correlation tracking requires stable, high-resolution sequences of images, which is possible with AO corrected NST NIR observations. The results from our NIR observations will be compared with visible observations from Hinode and SDO.

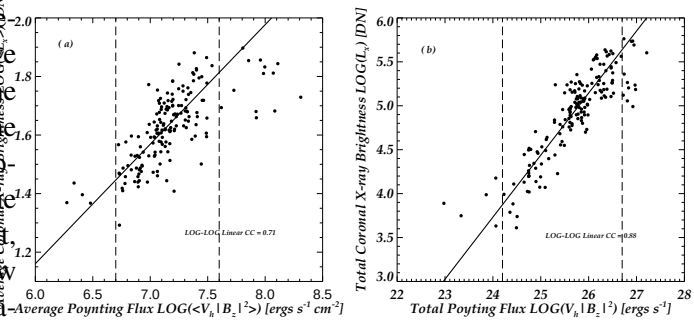

Figure 5: (a) Area-averaged and (b) area-integrated scatter plots showing the log-log correlation between Poynting flux and coronal X-ray brightness. Solid lines show first-degree polynomial fits to the data. Vertical dashed lines outline the data used to calculate the linear fits and correlation coefficients (Tan et al., 2007).

B.2.3 Quantitative and Systematic Studies of the Evolution of Magnetic Fields Associated with Flares and CMEs

As we have discussed in §B.1, we have begun to understand the consistent pattern of changes in the magnetic fields in the core regions of flares and CMEs. The most outstanding changes are the detected decay of the penumbral structure on the outer part of δ-spots, and the enhancement of umbral sunspot structure near the flaring neutral lines (Liu et al. 2005). These results were statistically confirmed and characterized in an investigation of over 400 events (Chen et al., 2007). These consistent, rapid changes in magnetic fields associated with flares have also been observed by Sudol and Harvey (2005). We anticipate that the NST will advance us to an ultimate physi-

cal understanding of these phenomena because of the higher magnetic sensitivity in the NIR.

For the limited number of events studied, we also found that the magnetic shear near the flaring neutral lines may increase after the flares (Wang 1992; Wang & Tang 1993; Wang et al. 1994, 2002, 2004b; Liu et al. 2005). The shear angle is defined as the angular difference between the observed azimuthal angle of the transverse fields and that of the extrapolated potential fields (Hagyard et al. 1990). Most of the events studied so far were observed from BBSO. However, a shear angle increase was also reported using the HSO (China) vector magnetogram data of AR 6659 on June 6, 1991 during the X12 flare (Schmieder et al. 1994), and the Marshall Space Flight Center (MSFC) vector magnetogram data of the famous AR 10486 on October 29, 2003 during an X10 flare (Liu et al. 2005). Figure 6 shows another recent example of transverse field enhancement along the flaring neutral line (from September 13, 2005 data, Wang et al., 2007).

As the observational evidence is solid, the scientific objective of this part of the proposed research is straightforward: to understand the physics of the observed magnetic field changes. For this, one requires high-cadence, high-resolution and highly stable vector magnetograms. *Obviously, due to the stability of the terrestrial atmosphere and line formation height in the lower photosphere at wavelengths near the opacity minimum at 1.6 μm, IRIM on the AO-76 equipped NST will be ideally suited for the purpose of probing the underlying physics of magnetic field changes arising from impulsive events.* Depending on the number of spectral positions chosen for the line scans in IRIM operations, we will have a few minute cadence for vector magnetograms. The expected polarization accuracy will be our nominal 10^{-3}. The spatial resolution will be around $0.2''$ for direct imaging, and $0.4''$ for magnetograms. Using the well-calibrated IRIM data, we will target the following two topics that we couldn't address before: **(1) the structure of full vector fields after correction for geometric projection; (2) the spectroscopic properties of the areas undergoing rapid structural changes to reveal the temperature and density changes.**

We recognize that accumulating data on flare events will take some time. Therefore, we will initially use the rich archive of BBSO vector magnetograms that

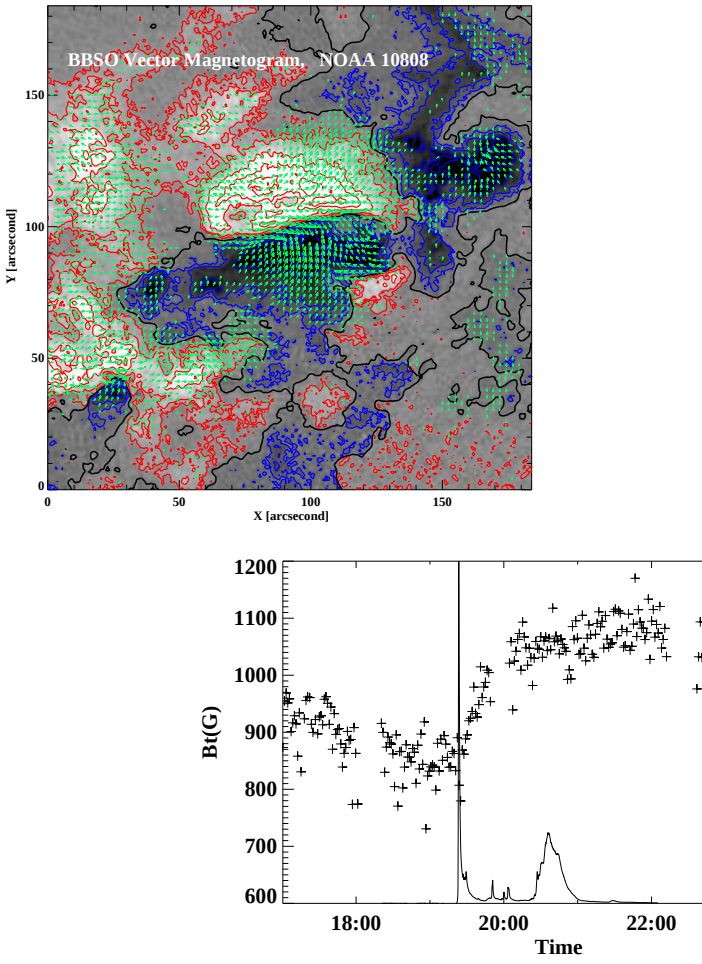

Figure 6: Top: A BBSO vector magnetogram of September 13, 2005. Bottom: The time profile of the mean transverse field strength in the section of the neutral line close to the initial flare core. The timing of the flare is indicated by the 10 GHz OVSA microwave light curve (solid line Wang et al. 2007).

covers almost 10 years of observations. With new and old data, we will fully develop data analysis tools, while gaining physical insight through analyzing the data, even if the 50 to 100 archived events would represent inferior data to those which will come from the NST. Obviously, this work on archived data would be further motivated in case of any delay in the NST.

In parallel, vector magnetograph data should be obtained by the recently launched Hinode. Joint Hinode/NST observations will be complementary: NST observes magnetic fields in the NIR, while Hinode operates mainly in the visible; the NST has a much larger aperture, while Hinode has continuous seeing-free coverage. The high-cadence observations from

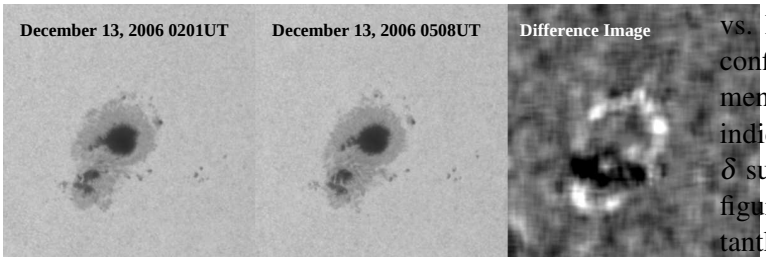

Figure 7: Left: TRACE WL image at 0201 UT before the onset of the X3.4 flare on December 13, 2006. Middle: WL image after the flare at 0508 UT. Right: the difference between post- and preflare WL intensity. The peripheral penumbral decay is evident from the bright ring in the difference image, while the enhancement of sunspot structure at the flaring neutral line is seen as a dark band.

the Hinode filtergraph observations are essential to detect and characterize the rapid structural changes in sunspots. However, Hinode has some technical difficulties that preclude vector magnetograph observations at this writing. On the other hand, analyzing lower-cadence Hinode spectro-polarimeter observations will enable us to study spectral line profiles in the areas that sustain structural changes. Therefore, we can come to understand more detailed physical characteristics (e.g., temperature, density and more accurate polarimetry) of the rapid changes in active region structure associated with flares.

In December 2006, Hinode obtained excellent coverage of AR 10930 that produced 3 X-class flares. Figure 8 shows the before and after TRACE WL images and their difference image around the X3.4 flare. It is obvious that this region shows similar properties to other events studied by us before: enhancement of sunspot structure at the flaring neutral line, and peripheral penumbral decay. From two vector magnetograms covering the X3.4 flare, we can see that the decrease in, and increase in transverse fields after the flare are quite obviously associated with the peripheral penumbra decay and central feature enhancement regions, respectively. Again, analysis of Hinode data will help us to develop data analysis tools that will be applied to NST high-resolution data.

After analyzing a large number of events, we will determine the physical differences between the regions with and without rapid changes in magnetic fields. The essential factors could include impulsive vs. long-duration events, sigmoidal or non-sigmoidal configurations, δ or non-δ configurations, and filament eruption association or not. Preliminary results indicate that the field changes are more detectable in δ sunspots, and when associated with sigmoidal configuration and long-duration flares. Even more importantly, the observations will be used to test a variety of flare models. For example, Wang et al. (2006) have demonstrated that the observed change of magnetic structure can be well-explained by the tether cutting model (Moore et al., 2001).

Furthermore, we are collaborating with a few groups to carry out non-linear force-free extrapolations in order to understand the evolution of the three-dimensional structure of magnetic fields associated with flares. The most notable work is our collaboration with Thomas Wiegelmann (Jing et al., 2008). Schrijver et al. (2006) compared the results of a number of leading NLFF extrapolation codes, and concluded that the optimization algorithm implemented by Wiegelmann is the fastest-converging and best-performing model. Recently, substantial progress has been made by the community in handling a difficult problems in analyzing vector magnetograms: to resolve the 180 degree ambiguity in the transverse fields (Metcalf et al. 2006). Therefore, NLFF extrapolation as formulated above will be extremely useful to study 3-D magnetic fields from photosphere to corona. Figure 8 shows NLFF extrapolation results for the two Hinode vector magnetograms covering the flare on December 13, 2006. Changes in magnetic field structure are quite obvious. In a more careful study using these extrapolations, Jing et al. (2008) found that magnetic shear increases in the lower atmosphere, while decreasing substantially in the higher atmosphere.

B.2.4 Surface Flows of Flare Producing Active Regions

In addition to finding permanent changes in magnetic fields associated with flares, we recently found another important and related phenomenon: rapid changes in flow patterns associated with flares. Figure 9 shows the very first clear demonstration of the shear flow of an active region before flaring, in particular before the X10 flare on October 29, 2003. We note that these observations were taken using the BBSO visible and NIR imaging systems. With the aid

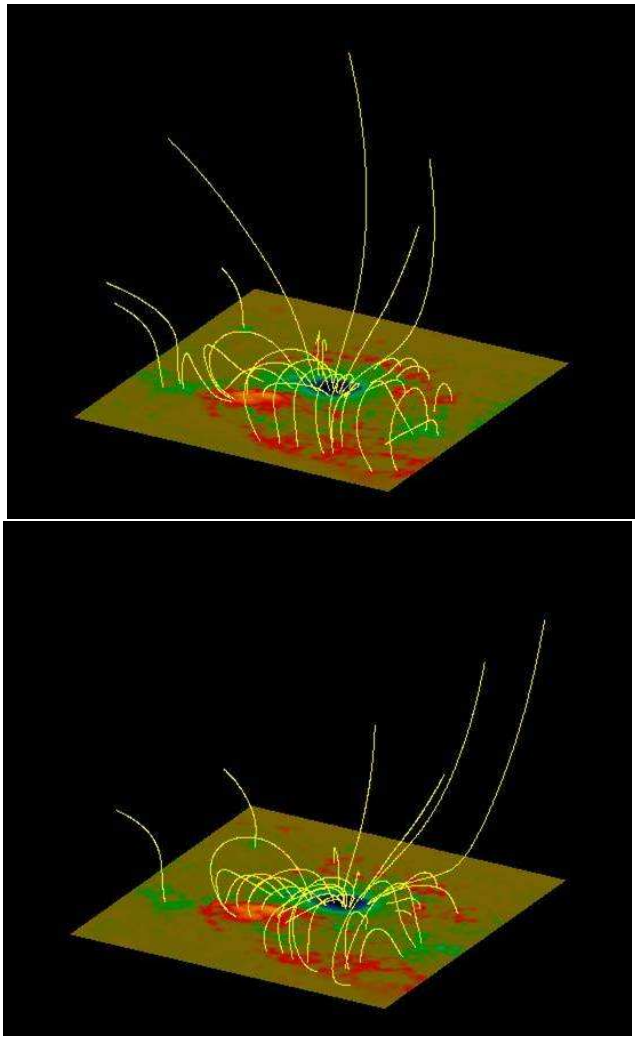

Figure 8: Comparison of NLFF extrapolation for two Hinode vector magnetograms, at 20:30 UT on December 12 and 04:30 UT on December 13, 2006, respectively. One was observed before and one after the X3.4 flare occurred at 02:40 UT on December 13 (courtesy Dr. Thomas Wiegelmann) .

of the AO system on the Dunn Telescope, diffraction-limited images were obtained with high-cadence, and they were analyzed carefully. The shear flows are very obviously associated with flaring neutral lines (Yang et al. 2004; Deng et al. 2006). Deng et al. (2006) also found that the shear flow increased after the onset of a flare. This is the only sub-arcsec, X-class, WL flare observation in existence, and it was covered completely with $0.2''$ resolution in WL. In the NST era with all the advantages of the NIR, this precision of flare observation will not be unusual. The tools that we developed over the last few years to study the flow fields will be readily applied to the NST data when available.

To observe these flows and magnetic field structures in detail and to understand their basic nature, we need high-resolution and high-cadence observations. Obviously, the AO equipped NST will attain the required higher resolution by finally advancing us beneath the $0.1''$ resolution limit in visible light. In our planned studies, we expect to answer the following questions: **(1) Do active regions always show changes in flows associated with flaring as discussed above? What are the spatial distributions of the flow evolution? (2) Are shear flows unusually strong before a major flare, and spatially located close to the flaring neutral line? (3) What are the physical implications of shear relaxation on large-scales and shear increase in a small area near the flaring neutral line (Wang, 2006)?** Again, observational results will be compared with flare/CME models that require formation of sheared magnetic fields by shear motion, such as the break-out model (Antiochos 1998; Antiochos et al. 1999). Complementary to NST data, Hinode data will provide high polarization accuracy, while SDO will provide full disk coverage of vector magnetograms.

C. Personnel and Management

Name	Role	Tasks
Goode	PI	Overall Supervis
Wang	Co-I	Coordination of
Cao	Co-I	Focal Plane Instr
Liu	Post-doc	Evolution of Ma
Valentina Abramenko	Researcher	Active Region F
Fear	Senior Observer	NST Observatio
Graduate Student		Flare Studies
Varsik, Shumko, Abramenko	Staff	Instrumentation

Table 2: Role and Tasks of Team Members

To develop state-of-the-art instrumentation and carry out the frontier research with our precious resources, we must have a balanced, first-class instrumentation and science teams. Three regular professors will have their own distinct but linked responsibilities (see Table 2). The research and instrumentation teams are also identified in the table. *What we*

propose is very cautious because if the NST's scientific operation has unforeseen delays, BBSO can still deliver scientific results: (1) Our IRIM and VIM system can be used at NSO/SP as we have done in the last few years. (2) Our global Hα network has 6 stations for full disk observations, plus one station in China for high-cadence flare observations. (3) Many data analysis tools developed can be applied to NASA mission data easily. (4) BBSO has a rich data archive.

For the early part of the first year when we finish integrating the NST, more resources will be devoted to instrumentation. Starting in the middle of the first year, scientific research using the NST will become the dominant effort.

D. References Cited

Antiochos, S. K., 1998, *The Magnetic Topology of Solar Eruptions*, Ap. J. Letters, 502, L181-L184

Antiochos, S. K., DeVore, C. R., & Klimchuk, J. A., 1999, *A Model for Solar Coronal Mass Ejections*, Ap. J., 510, 485-493

Aschwanden, M. J. 2002, Particle Acceleration and Kinematics in Solar Flares, Kluwer Academic Publishers

Aschwanden, M. J., Schwartz, R. A., & Alt, D. M., 1995, *Electron Time-of-Flight Differences in Solar Flares*, Ap.J., 447, 923-935

Aschwanden, M. J., Benz, A. O., & Schwartz, R. A., 1993, *The Timing of Electron Beam Signatures in Hard X-Ray and Radio: Solar Flare Observations by BATSE/Compton Gamma-Ray Observatory and PHOENIX*, Ap.J., 417, 790-804

Aschwanden, M. J., Benz, A. O., Dennis, B. R., & Schwartz, R. A., 1995, *Solar Electron Beams Detected in Hard X-Rays and Radio Waves*, Ap.J., 455, 347-365

Aschwanden, M. J., Kliem, B., Schwarz, U., Kurths, J., Dennis, B. R., & Schwartz, R. A., 1998, *Wavelet Analysis of Solar Flare Hard X-Rays*, Ap.J., 505, 941-956

Aschwanden, M. J., Nightingale, R. W., Alexander, D., 2000, *Evidence for Nonuniform Heating of Coronal Loops Inferred from Multithread Modeling of TRACE Data*, Ap.J., 541, 1059-1077

Bastian, T. S., & Vlahos, L. 1997, in "Coronal Physics and Space Observations", ed. Trottet, p. 68

Benka, S. G., & Holman, G. D. 1994, *A Thermal/nonthermal Model for Solar Hard X-ray Bursts*, Ap.J., 435, 469-481

Cao, W., Jing, J., Ma J., Xu, Y., Wang, H. & Goode, P.R., 2006, *Diffraction-limited Polarimetry from the Infrared Imaging Magnetograph at Big Bear Solar Observatory*, PASP, 118, 838-844

Carmichael, H. 1964, in Proc. AAS-NASA Symp., The Physics of Solar Flares, ed. W. N. Hess (Washington, DC: NASA), 451

Chen, W., Liu, C., & Wang, H., 2007, *Statistical Study of Rapid Penumbral Decay Associated with Flares*, ChJAA., in press,

de Jager, C. & de Jonge, G. 1978, *Properties of Elementary Flare Bursts*, Solar Physics, 58, 127-137

Deng, N., Liu, C., Yang, G., Wang, H., & Denker, C., 2005, *Rapid Penumbral Decay Associated with An X2.3 Flare in NOAA Active Region 9026*, Ap. J., 623, 1195-1201

Deng, N., Xu, Y., Yang, G., Cao, W., Liu, C., Rimmele, T. R., Wang, H., & Denker, C., 2006, *Multiwavelength Study of Flow Fields in Flaring Super Active Region NOAA 10486*, Ap. J., 644, 1278-1291

Denker, C., Yang, G., & Wang, H., 2001, *Near Real-Time Image Reconstruction*, Solar Physics, 202, 63-70

Denker, C., Mascarinas, D., Xu, Y. Cao, W., Yang, G., Wang, H., Goode, P. R. and Rimmele, T., 2005, *High-Spatial-Resolution Imaging Combining High-Order Adaptive Optics, Frame Selection, and Speckle Masking Reconstruction*, Solar Physics, 227, 217-230

Denker, C., Tritschler, A., Rimmele, T. R., Richard, K., Hegwer, S. L. & Woger, F., 2007, *Adaptive Optics at the Big Bear Solar Observatory: Instrument Description and First Observations*, PASP, 119, 170-182

Didkovsky, L, Dolgushyn, A., Marquette, W., Hegwer, S., Ren, D. Fletcher, S. Richards, K., Rimmele, T. R. Denker, C. and Wang, H. 2003, *High-order Adaptive Optical System for Big-Bear Solar Observatory*, Proc. SPIE, 4853, 630-639

Ding, M. D., Qiu, J., Wang, H., & Goode, P. R. 2001, *On the Fast Fluctuations in Solar Flare Ha Blue Wing Emission*, Ap.J., 552, 340-347

Forbes, T. G., & Priest, E.R., 1995, *Photospheric Magnetic Field Evolution and Eruptive Flares*, Ap.J., 446, 337-389

Fu, G., Shih, F.Y. & Wang, H., 2007, *Automated Detection of Filament Eruptions*, IEEE Trans on CSVT, 17, 79-85

Hagyard, M. J., Venkatakrishnan, P., & Smith, J. B., Jr., 1990, *Nonpotential Magnetic Fields at Sites of Gamma-Ray Flares*, Ap. J. Suppl. 73, 159-163

Harvey, J. W., Branston, D., Henney, C. J. & Keller, C. U., 2007, *Seething Horizontal Magnetic Fields in the Quiet Solar Photosphere*, Ap.J. Letters, 659, L177-180

Hirayama, T. 1974, *Theoretical Model of Flares and Prominences. I: Evaporating Flare Model*, Sol. Phys., 34, 323-338

Hoyng, P., van Beek, H. F. & Brown, J. C., 1976, *High time resolution analysis of solar hard X-ray flares observed on board the ESRO TD-1A satellite*, Solar Physics, 48, 197-254

Hudson, H.S., 1991, *Solar flares, microflares, nanoflares, and coronal heating*, Solar Physics, 133, 357-369

Hudson, H. S., 2000, *Implosions in Coronal Transients*, Ap.J. Letters, 531, L75-78

Ji, H., Wang, H., Schmahl, E. J., Moon, Y. & Jiang, Y., 2003, *Observations of the Failed Eruption of a Filament*,Ap.J. Letters, 597, L161-164

Ji, H., Wang, H., Schmahl, E. J., Qiu, J. & Zhang, Y., 2004a, *Observations of Nonthermal and Thermal Hard X-Ray Spikes in an M-Class Flare*, Ap. J., 605, 938-947

Ji, H., Wang, H., Goode, P. R., Jiang, Y., Yurchyshyn, V., 2004b, *Traces of the Dynamic Current Sheet during a Solar Flare*, Ap.J. Letters, 607, L55-58

Ji, H., Huang, G., Wang, H., Zhou, T., Li, Y., Zhang, Y. & Song, M., 2006, *Converging Motion of Hα Conjugate Kernels: The Signature of Fast Relaxation of a Sheared Magnetic Field*, Ap.J. Letters, 636, L173-176

Jing, J., Yurchyshyn, V. B., Yang, G., Xu, Y. & Wang, H., 2004, *On the Relation between Filament Eruptions, Flares, and Coronal Mass Ejections*, ApJ, 614, 1054-1062

Jing, J., Qiu, J., Lin, J., Qu, M., Xu, Y. & Wang, H., 2005, *Magnetic Reconnection Rate and Flux-Rope Acceleration of Two-Ribbon Flares*, ApJ, 620, 1085-1091

Jing, J., Lee, J., Liu, C., Gary, D.E. & Wang, H., 2007, *Hard X-ray Intensity Distribution Along Hα Ribbons*, Ap.J. Letters, 644, L127-130

Jing, J., Wiegelmann, T., Suematsu, Y., Kubo, M. & Wang, H., 2008, *Changes of Magnetic Structure in 3-D Associated with the X3.4 Flare of 2006 December 13*, Ap.J. Letters, submitted

Kaufmann, P., Strauss, F. M., Laporte, C., & Opher, R. 1980, *Evidence for quasi-quantization of solar flare mm-wave radiation*, A&A, 87, 58-62

Kaufmann, P., Correia, E., Costa, J. E. R., Dennis, B. R., Hurford, G. J., & Brown, J. C. 1984, *Multiple energetic injections in a strong spike-like solar burst*, Sol. Phys., 91, 359-376

Kaufmann, P., Raulin, J.-P., Correia, E., Costa, J. E. R., de Castro, C. G. Gimenez, Silva, A. V. R., Levato, H., Rovira, M., Mandrini, C., Fernandez-Borda, R., & Bauer, O. H., 2001, *Rapid Submillimeter Brightenings Associated with a Large Solar Flare*, Ap.J. Letters, 548, L95-98

Kiplinger, A. L., Dennis, B. R., Emslie, A. G., Frost, K. J., & Orwig, L. E., 1983, *Millisecond time variations in hard X-ray solar flares*, Ap.J., 265, L99-104

Kiplinger, A. L., Dennis, B. R., Orwig, L. E., & Chen, P. C. 1988, Proc. First Max'91 Workshop, Kansas City, p. 214

Kliem, B., Karlicky, M. & Benz, A.O., *Solar flare radio pulsations as a signature of dynamic magnetic reconnection*, 2000, A&A, 360, 715-728

Kopp, R. A. & Pneuman, G. W. 1976, *Magnetic reconnection in the corona and the loop prominence phenomenon*, Sol. Phys., 50, 85-98

Kurt, V. G., Akimov, V. V., Hagyard, M. J., & Hathaway, D. H. 2000, in Ramaty, R. & Mandzhavidze, N. (eds.) High Energy Solar Physics: Anticipating HESSI, ASP Conference Series, Vol. 206, p. 426

Lites, B.W., et al., 2008, Ap.J., 672, 1237

Liu, C., Deng, N., Liu, Y., Falconer, D., Goode, P. R., Denker, C., & Wang, H., 2005, *Rapid Change of δ Spot Structure Associated with Seven Major Flares*, Ap. J., 622, 722-736

Liu, C., Lee, J., Gary, D. E. & Wang, H., 2007, *The Ribbon-like Hard X-Ray Emission in a Sigmoidal Solar Active Region*, Ap.J. Letter, 658, L127-130

Lu, E. T., & Hamilton, R. J. 1991, *Avalanches and the distribution of solar flares*, Ap.J. Letters, 380, L89-92

Moore, R.L., Sterling, A.C., Hudson, H.S., & Lemen, J., 2001, *Onset of the Magnetic Explosion in Solar Flares and Coronal Mass Ejections*, Ap.J., 552, 833-848

Parker, E.N., 1988, *Nanoflares and the solar X-ray corona*, Ap.J., 330, 474-479

Parker, E. N. 1989, *Solar and stellar magnetic fields and atmospheric structures - Theory*, Sol. Phys., 121, 271-288

Priest, E. R., Foley, C. R., Heyvaerts, J., Arber, T. D., Mackay, D., Culhane, J. L. & Acton, L. W., 2000, *A Method to Determine the Heating Mechanisms of the Solar Corona*, Ap.J., 539, 1002-1022

Qiu, J. & Wang, H., 2006, *On the Temporal and Spatial Properties of Elementary Bursts*, Solar Physics, 236, 293-311

Qiu, J., Ding, M., Wang, H., Denker, C., & Goode, P. R., 2000, *Ultraviolet and Ha Emission in Ellerman Bombs*, Ap.J. Letters, 544, L157-160

Qiu, J., Ding, M. D., Wang, H., Gallagher, P. T., Sato, J., Denker, C., & Goode, P. R. 2001, *Asymmetric Behavior of Ha Footpoint Emission during the Early Phase of an Impulsive Flare*, ApJ, 554, 445-450

Qiu, J., Lee, J., Gary, D. E., & Wang, H. 2002, *Motion of Flare Footpoint Emission and Inferred Electric Field in Reconnecting Current Sheets*, ApJ, 565, 1335-1347

Qu, M., Shih, F. Y., Jing, J. & Wang, H., 2003, *Automatic Solar Flare Detection Using MLP, RBF, and SVM*, Sol. Phys., 217, 157-172

Qu, M., Shih, F. Y., Jing, J. & Wang, H., 2004, *Automatic Solar Flare Tracking Using Image-Processing Techniques*, Sol. Phys., 222, 137-149

Qu, M., Shih, F. Y., Jing, J. & Wang, H., 2005, *Automatic Solar Filament Detection Using Image Processing Techniques*, Sol. Phys., 228, 119-135

Qu, M., Shih, F. Y., Jing, J. & Wang, H., 2006 *Automatic Detection and Classification of Coronal Mass Ejections*, Sol. Phys., 237, 419-431

Ren, D., Hegwer, S. and Rimmele, T. R. et al. 2003, *The Optical Design of a High Order Adaptive Optics for the NSO Dunn Solar Telescope and the Big Bear Solar Observatory*, Proc. SPIE, 4853, 593

Rimmele, T. R., 2004 *Recent advances in solar adaptive optics*, 2004, SPIE, 5490, 34

Rimmele, T. R., 2008, private communication

Schmieder, B., Hagyard, M. J., Ai, G., Zhang, H., Kalman, B., Gyori, L., Rompolt, B., Demoulin, P., & Machado, M. E., 1994, *Relationship Between Magnetic Field Evolution and Flaring Sites in AR 6659 in June 1991*, Solar Physics, 150, 199-219

Sturrock, P. A. 1966, *Model of the High-Energy Phase of Solar Flares*, Nature, 211, 695-697

Sturrock, P. A., Kaufman, P., Moore, R. L. & Smith, D. F. 1984, *Energy release in solar flares*, Solar Phys., 94, 341-357

Suarez, D. et al., 2007, *Quiet-Sun Internetwork Magnetic Fields from the Inversion of Hinode Measurements*, Ap.J. Letters, 670, L61-64

Sudol, J. J., & Harvey, J. W., 2005, *Changes in the Longitudinal Magnetic Field during Solar Flares*, Ap. J., 635, 637-658

Sui, L. & Holman, G.D., 2003, *Evidence for the Formation of a Large-Scale Current Sheet in a Solar Flare*, Ap.J. Letters, 596, L251-254

Sui, L., Holman, G.D. & Dennis, B.R., 2004, *Evidence for Magnetic Reconnection in Three Homologous Solar Flares Observed by RHESSI*, Ap.J, 612, 546-556

Svestka, Z., & Cliver, E. W. 1992, in IAU Colloq. 133, Eruptive Flares, ed. Z. vestka, B. V. Jackson & M. E. Machado (New York: Springer), 1

Tan, C., Jing, J., Abramenko, V., Pevtsov, A. A., Song, H., Park, S.H. & Wang, H., 2007, *Statistical Correlations between Parameters of Photospheric Magnetic Fields and Coronal Soft X-Ray Brightness*, Ap.J., 665. 1460-1468

Trottet, G., Rolli, E., Magun, A., Barat, C., Kuznetsov, A., Sunyaev, R., & Terekhov, O. 2000, *The fast and slow Hα chromospheric responses to non-thermal particles produced during the 1991 March 13 hard X-ray/gamma-ray flare at 08 UTC*, A&A, 356, 1067-1075

van Beek, H. F., de Feiter, L. D., & de Jager, C. 1974, In: Space research XIV; Proceedings of the Sixteenth Plenary Meeting, Berlin, East Germany, Akademie-Verlag GmbH, p. 447

van Beek, H. F., de Feiter, L. D., & de Jager, C. 1976, In: Space research XVI; Proceedings of the Open Meetings of Working Groups on Physical Sciences, Berlin, East Germany, Akademie-Verlag GmbH, p. 819

Veronig, A.M., Karlicky, M., Vrsnak, B., Temmer, M., Magdalenic, J., Dennis, B.R., Otruba, W. & Potzi, W., 2006, *X-ray sources and magnetic reconnection in the X3.9 flare of 2003 November 3*, A&A, 446, 675-690

Wang, H., 1992, *Evolution of Vector Magnetic Fields and the August 27 1990 X-3 Flare*, Solar Physics, 140, 85-98

Wang, H., & Tang, F., 1993, *Flux Emergence and Umbra Formation After the X-9 Flare of 1991 March 22*, Ap. J. Letters, 407, L89-L90

Wang, H., & Qiu, J. *Relationship between Flare Kernels in Ha Far-Blue Wing and Magnetic Fields*, 2002, Ap.J., 568, 408-412

Wang, H., Ewell, M. W., Zirin, H., & Ai, G., 1994, *Vector Magnetic Field Changes Associated with X-class Flares*, Ap. J., 424, 436-443

Wang, H., Qiu, J., Denker, C., Spirock, T., Chen, H., & Goode, P. R. 2000, *High-Cadence Observations of an Impulsive Flare*, Ap.J., 542, 1080-1087

Wang, H., Gallagher, P., Yurchyshyn, V., Yang, G., & Goode, P. R., 2002, *Core and Large-Scale Structure of the 2000 November 24 X-Class Flare and Coronal Mass Ejection*, Ap. J., 569, 1023-1031

Wang, H., Liu, C., Qiu, J., Deng, N., Goode, P. R., & Denker, C., 2004a, *Rapid Penumbral Decay Following Three X-Class Solar Flares*, Ap. J. Letters, 601, L195-L198

Wang, H., Qiu, J., Jing, J., Spirock, T. J., Yurchyshyn, V., Abramenko, V., Ji, H., & Goode, P. R., 2004b, *Evidence of Rapid Flux Emergence Associated with the M8.7 Flare on 2002 July 26*, Ap. J., 605, 931-937

Wang, H., 2006, *Rapid Changes of Magnetic Fields around Flaring Neutral Lines*, Ap.J., 649, 490-497

Wedemeyer-Bohm, S., Kamp, I, Bruls, J. & Freytag, B., 2005, *Carbon Monoxide in the Solar Atmosphere. I. Numerical Method and Two-Dimensional Models*, A&A, 438, 1043-1057

Xu, Y., Cao, W. Liu, C., Yang, G., Qiu, J., Jing, J., Denker, C. & Wang, H., 2004, *Near-Infrared Observations at 1.56 Microns of the 2003 October 29 X10 White-Light Flare*, Ap.J. Letters, 607, L131-134

Xu, Y., Cao, W. Liu, C., Yang, G., Jing, J., Denker, C., Emslie, G. A. & Wang, H., 2006, *High-Resolution Observations of Multiwavelength Emissions during Two X-Class White-Light Flares*, Ap.J., 641, 1210-1216

Yang, G., Xu, Y., Cao, W., Wang, H., Denker, C., & Rimmele, T. R., 2004, *Photospheric Shear Flows Along the Magnetic Neutral Line of Active Region 10486 Prior to An X10 Flare*, 2004, Ap. J. Letters, 617, L151-L154

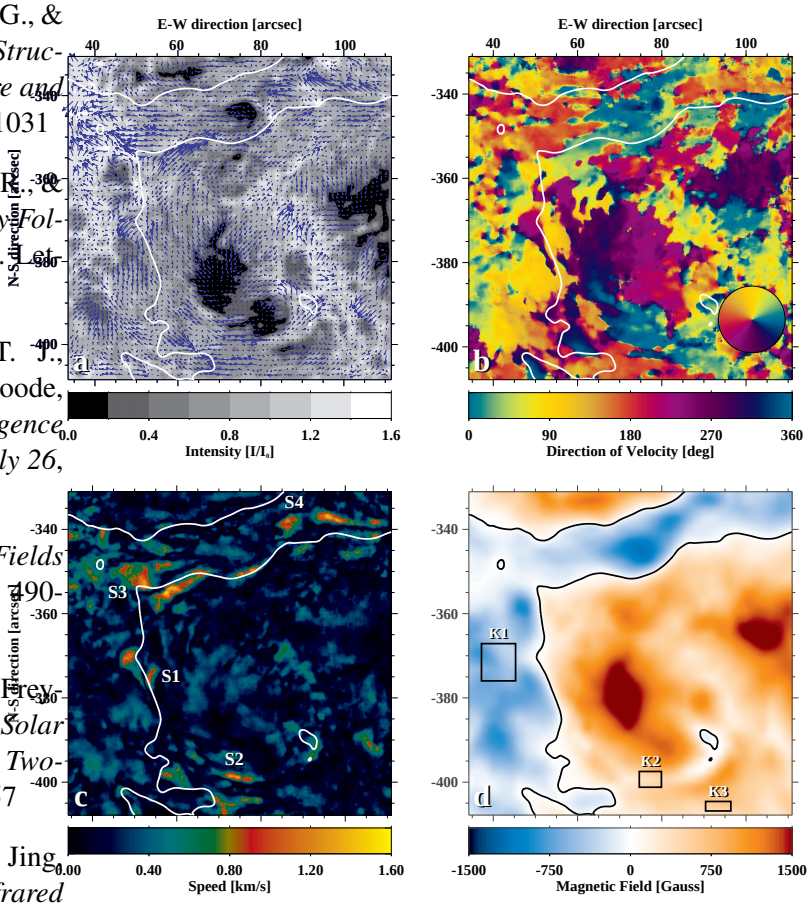

Figure 9: Photospheric flows and magnetic field configuration of NOAA 10486 on October 29, 2003. To illustrate the results of high spatial resolution local correlation tracking analysis of WL data observed by the BBSO team at NSO/SP, we show different views of (a) flow vectors, (b) azimuthal angle of the velocity vectors, (c) magnitude of the velocity vectors, and (d) MDI magnetogram with superimposed magnetic neutral lines. I/I_0 in (a) is the normalized intensity relative to quiet photosphere (Yang et al. 2004). Strong shear flows are found along flaring neutral line, denoted by S1 through S4; while K1 through K3 mark flare kernels.